On evaluating the efficacy of air-borne synthetic aperture radar for detecting polar bears: A pilot study

Authors: George, Brent, Bateman, Terri, Formica, Mckay, Gronnemose, Wyatt, Hilke, Nicholas, et al.

Source: Ursus, 2023(34e6) : 1-17

Published By: International Association for Bear Research and Management

URL: https://doi.org/10.2192/URSUS-D-22-00018

On evaluating the efficacy of air-borne synthetic aperture radar for detecting polar bears: A pilot study

Brent George[1], Terri Bateman[1], Mckay Formica[1], Wyatt Gronnemose[2], Nicholas Hilke[1], Usman Iqbal[2], B.J. Kirschoffer[3], Bernhard Rabus[2], Tom Smith[1], Jeff Stacey[2], Lucas Stock[1], Evan Zaugg[4], and David Long[1,5]

[1]*Brigham Young University, Provo, UT 84604, USA*
[2]*Simon Fraser University, Burnaby, BC V5A 1S6, Canada*
[3]*Polar Bears International, Bozeman, MT 59772, USA*
[4]*Artemis, Inc., Haupauge, NY 11788, USA*

Abstract: Knowing the location of polar bears (*Ursus maritimus*) in their winter dens is crucial for minimizing disturbance during this critical period in their life cycle. Previous research has used Forward Looking Infrared (FLIR) technology to detect bear dens but has only achieved a detection accuracy of 45% for single flights. The thermal nature of FLIR means that some bears are never detected nor are detectable using FLIR. In this paper we explore the use of Synthetic Aperture Radar (SAR) as an alternative polar bear detection technology in a simple pilot study in Churchill, Manitoba, Canada, during October 2021. In this experimental study, we focused on the detection of polar bears on the surface in the SAR images. The result of this study can inform future efforts to proceed to den-detection experiments. In this study, we achieved a polar bear identification accuracy of 66%, albeit with a small sample size. Many of the challenges we encountered involved low signal-to-noise ratios and imprecise flight paths. Concurrent research from other parties shows that neural networks and other machine learning techniques can overcome these challenges to some degree, suggesting that SAR may be a promising candidate to become an effective tool for polar bear detection, particularly when coupled with other sensors such as FLIR.

Key words: backscatter, bear, detection, polar bear, SAR, synthetic aperture radar, techniques, *Ursus maritimus*

DOI: 10.2192/URSUS-D-22-00018 ***Ursus 34:article e6 (2023)***

Denning is the most vulnerable time in a polar bear's (*Ursus maritimus*) life (Durner and Atwood 2018). During this time, polar bears are buried in snow and ice on all sides, making it virtually impossible to detect them without special equipment. Currently, the most common approach is to use Forward Looking Infrared (FLIR) cameras to detect polar bears via their heat signature. However, even when conditions are optimal, the detection rate is capped at ∼45% for single flights (Amstrup et al. 2009, Pedersen et al. 2020, Smith et al. 2020, Woodruff et al. 2022). As an alternative, Synthetic Aperture Radar (SAR) has been suggested as a possible tool to improve polar bear den detection because the SAR signal penetrates snow and ice layers and detects buried objects by observing the radar signal reflected from them (Ulaby and Long 2014).

The purpose of this paper is to briefly describe an experiment of opportunity to use air-borne SAR to detect polar bears on the surface. This pilot study serves as an initial validation step before conducting future work to use SAR to detect polar bears in their dens. To this end, we conducted an experiment in Churchill, Manitoba, Canada, in October 2021 to determine whether polar bears could be detected via SAR while they were on the surface. This experimental study explicitly uses specific choices for SAR polarization, channels, flight patterns, and other factors that would theoretically transfer to detecting polar bears not just on the surface but in their dens.

Polar bears are visible in SAR images because of their geometry and their contrast with the terrain. Change detection, where a SAR image is taken of the same area at 2 different times and compared, is a particularly effective tool in identifying targets that can move. Figure 1 shows an ideal example of how change detection may be applied to find a polar bear den in a noisy environment.

A large polar bear population gathers in Churchill every autumn while waiting to move onto the sea ice (Deocher and Stirling 1990, Stirling et al. 2004, Regehr

[5]email: long@byu.edu

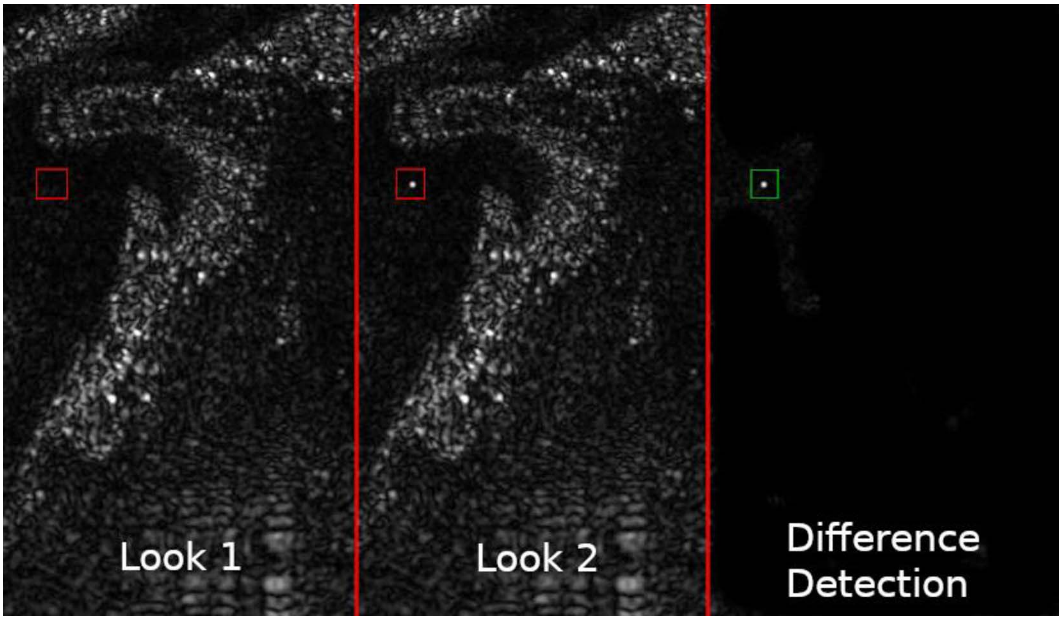

Fig. 1. Synthetic example of Synthetic Aperture Radar (SAR) image change detection. Look 1 (left panel) and Look 2 (center panel) represent SAR images taken at different times. The underlying terrain, including rocks and other geographic features, creates a nearly identical pattern in both images. These matching features from the looks are filtered out in the difference image shown in the right panel. The green box highlights a change between the 2 images resulting from the presence of a polar bear (*Ursus maritimus*). The red boxes show the same area in the input images.

et al. 2010, Pedersen et al. 2020). This behavioral reliability combined with the area's close proximity to human development has resulted in a well-studied and concentrated polar bear population, with many bears within a few square kilometers (Dyck and Baydack 2004). Researchers actively track bears in the area. This makes Churchill a good location for an initial pilot study. Further, the area is easy to access and flight lines could be planned for specific areas known to have polar bears, thus avoiding the possibility of imaging a large area and not capturing any polar bears. Knowing the actual locations of several bears in advance from tundra buggy observations enabled us to rigorously evaluate our methods in real time and quickly determine true positives, false positives, and false negatives.

Our Churchill study described below produced a bear detection accuracy of 66% with a sample size of 9 bears. Although this is a small sample set, our experiment is the first known documented use of SAR to detect polar bears from aircraft. Our prescribed methodology described below is a combination of what we did and suggested improvements for future experiments. A later section describes the SAR image analysis, including the challenges that stemmed from limitation of this specific study, as well as those inherent to SAR imaging.

Synthetic Aperture Radar versus Forward Looking Infrared

Unlike a FLIR or an optical camera, SAR is an active sensor (i.e., includes its own illumination source) that operates independently of solar conditions. Forward Looking Infrared is based on infrared wavelengths and is highly influenced by temperature and weather conditions common to Arctic regions (Pedersen et al. 2020, Smith et al. 2020). On the other hand, SAR emits electromagnetic waves of varying lengths that have the potential to penetrate dry snowpack (Ulaby and Long 2014). In other words, a SAR image of snow-covered terrain can display the underlying terrain, passing through dry snow. This has obvious positive implications for den detection, especially when polar bears are under snowpack. Unlike FLIR, which has no special licensing requirements, an appropriate radar transmitter license is required for air-borne SAR operation. Current SAR systems typically cost more than FLIR systems.

Theory of polar bear detection with Synthetic Aperture Radar

A SAR transmits a series of radio pulses from a moving platform. The received echoes are computer-processed into images of the power reflected from each pixel, which depends on the roughness and electrical properties (the dielectric constant) of the surface. The SAR image pixels are defined by along-track and cross-track distance (range) from the radar (Ulaby and Long 2014). Liquid water has a much higher dielectric constant than those of ice or frozen terrain, so that water containing polar bears exhibits a dielectric contrast with the background. Further, using interferometric SAR imaging techniques (Moreira et al. 2013), SARs can directly measure topography. In theory, polar bears exhibit a dielectric and shape contrast that is distinct from the underlying topography (Moreira et al. 2013).

Our working hypothesis is that if polar bears can be detected on the surface with SAR, then SAR can be a launching pad for then detecting polar bears in their dens because the SAR signal can penetrate dry snowpack and reflect from buried objects. This has obvious positive implications for den detection, where polar bears can be under snowpack >1 m thick (Pedersen et al. 2020). The radar penetration depth depends on the SAR frequency or wavelength. We note that SAR does not penetrate liquid water, and snowpack penetration falls off rapidly with snow wetness.

Methods

Frequency band for Synthetic Aperture Radar

The choice of operating frequency is a fundamental trade-off for radar. Shorter wavelengths, which correspond to higher frequencies, can better detect smaller objects, increasing the ability to visualize finer details; but longer wavelengths, which correspond to lower frequencies, have better penetration capability in dry snow (Ulaby and Long 2014). Further, larger wavelengths can be more forgiving for SAR imaging in rough flying conditions than smaller wavelengths.

Radar is best able to detect targets that are larger than the size of its wavelength (Moreira et al. 2013). Commonly used SAR bands pass this criterion for polar bear detection. Looking forward to future den detection, any of the bands with wavelengths >20–30 cm should be able to penetrate the snow accumulated on top of denned bears.

A given SAR unit may only have hardware to support a small subset of the available frequency bands. The specific SAR unit used in our study was an Artemis SAR (Artemis, Inc., Haupauge, New York, USA) supplied by Simon Fraser University. Although it had the capability to operate at X-band (10 GHz) and L-band (1.6 GHz) frequencies, we would only use the L-band channels in this study because of a connector damaged in transit. Using the SAR we collected multipolarization images. Further research should be conducted with other frequency bands to compare detection performance among them.

Polarization for Synthetic Aperture Radar

Radars can use different electromagnetic signal polarizations. Polarization refers to the orientation of the electromagnetic field in the propagating radar wave front with respect to the surface. By varying the polarization of the transmitted signal and receiving several different polarized images from the same series of pulses, SAR systems can gather detailed information on the polarimetric properties of the observed surface, which can reveal information about the structure, orientation, and environmental conditions of the surface elements (Zyl and Kim 2011). In other words, different polarizations 'see' different things about the snow and land surfaces.

Flight platform

For our study, we mounted the SAR on a helicopter (see Fig. 2), though fixed-wing aircraft also can be used. The SAR antennas were mounted to a bar attached to the helicopter skids. To provide wide-area coverage, we use strip-map SAR imaging techniques (Ulaby and Long 2014). In strip-map SAR, optimal images are formed when the antenna illuminates an area orthogonal to the flight direction. Crosswinds result in aircraft yaw, which can adversely affect the quality of the SAR images (Roh et al. 2020). For a fixed-mount antenna, aircraft yaw changes the antenna pointing so that it is no longer orthogonal to the flight path, resulting in degraded imaging quality. This phenomenon is much more prevalent with a helicopter than a fixed-wing aircraft, so the pilot must maintain his heading to keep the SAR antenna pointing perpendicular to the desired flight line. Pilot skill and experience can make a large difference in final image quality.

Fixed-wing aircraft are able to fly at a higher elevation above fog and clouds, widening the swath width possible compared with helicopters, which typically fly lower and thus are more susceptible to local weather conditions (U.S. Department of Transportation, Federal Aviation Administration 2023). Fixed-wing aircraft can be cheaper to operate than helicopters but require additional safety certifications when attaching external equipment. For the Churchill experiment, availability considerations drove us to use a helicopter despite the advantages of a fixed-wing aircraft. Local cloud conditions in Churchill forced the helicopter to remain below 333 m (1,000 ft) in elevation during the study period.

Fig. 2. (top) Computer-aided design (CAD) rendering of the Synthetic Aperture Radar (SAR) antennas mounted on the helicopter. (bottom) Photograph of antennas mounted on helicopter. The SAR antennas are highlighted in red boxes. The SAR electronics are mounted in the cabin.

For this study, we attached a digital single-lens reflex camera adjacent to the SAR antenna. The camera acted as a 'fodar' (a portmanteau of 'foto' and 'lidar'; https://fairbanksfodar.com/understanding-fodar), a method of air-borne photogrammetry in which digital aerial photos can be used with recorded coordinates to produce a topographical map (Nolan et al. 2015). An intervalometer triggered the camera at a precise interval based on ground speed and altitude to produce an 80% overlap between subsequent images. The intervalometer also embedded timing in the data stream so the picture time was precisely recorded for comparison with the SAR imagery.

As previously noted, SAR enables measurement of surface backscatter independent of solar illumination. Further, when properly calibrated the backscatter measurements can be directly related to surface roughness and dielectric

Fig. 3. Deployed 122-cm (4 ft) corner reflector at the Churchill (Manitoba, Canada) site.

constant (Ulaby and Long 2014). Calibration also simplifies comparison of images taken at different times. In order to accurately calibrate SAR backscatter, we included a calibration corner reflector in a low interference area of the image (Doerry 2008). The corner reflector was imaged by the helicopter as part of the data collecting process. The corner reflector's radar signature is used to calibrate SAR and identify inconsistencies from flight to flight (Garthwaite et al. 2015). Ideal reflector geometries can vary depending on the frequency band, transportation requirements, and accuracy thresholds of the specific imaging process (Li et al. 2010). For this study, we employed a custom-designed 122-cm (4-ft) trihedral reflector that was secured and stiffened using ropes (see Fig. 3). The corner reflector appears at the center of the bright cross shape in Figure 4.

Flight lines

Flight line planning is critical to the success of the data collection. To plan and execute flight lines, we considered maximum and minimum flight height, potential

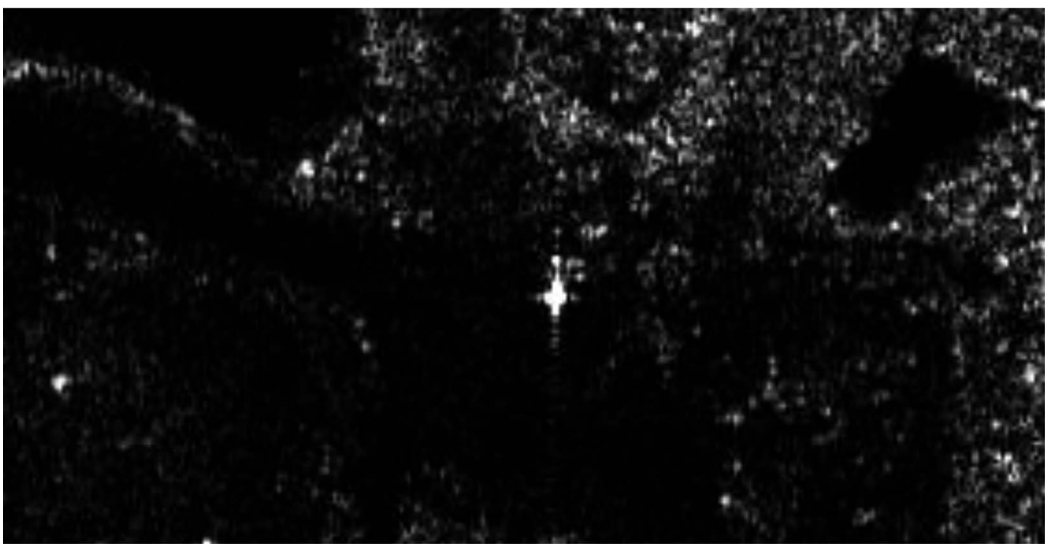

Fig. 4. The calibration corner reflector appears in the center of the image as a cross-like shape. The dots on the arms of the cross that result from sidelobes of the Synthetic Aperture Radar (SAR) impulse response provide radar-imaging experts with information on image quality and resolution.

bear locations, and the relationship between the total area mapped and the number of looks per area of interest. As the SAR unit flies higher above the ground, the swath width potentially increases but the resolution remains constant (Ulaby and Long 2014). The return power of the SAR signal decreases as flight height increases, which lowers the effective signal-to-noise ratio. The upper bound on SAR use is dictated by the maximum height at which the signal returned to the SAR is powerful enough to be distinct from background noise (Garthwaite et al. 2015). Based on previous experiments with the SAR hardware observing humans surrogates in snow caves, we empirically determined that an altitude of ~457 m (1,500 ft) reasonably balances swath width, imaging quality, and penetration power.

As previously noted, aircraft flights can be limited by visibility concerns from weather and low cloud cover. Local regulations may also limit the maximum altitude of a planned flight. In these cases, we planned several preprogrammed flight lines ahead of time in the same locations but at various altitudes. The proper flight line can be chosen in conjunction with the pilot, who can advise on weather conditions and other mitigating factors that affect the maximum altitude of the aircraft. Per government regulations in Manitoba, we had to maintain a minimum flight height of ~150 m (500 ft) to avoid bear disturbance.

Ideally, to ensure high-quality SAR images and avoid image distortion, particularly when doing change detection, flight lines should be as smooth and straight as possible when collecting data. Straight flight lines are also more easily repeated, a necessity for change detection. Other types of SAR flight lines, such as circular, can allow for more accuracy in imaging a known target using circular mode SAR (Ulaby and Long 2014), but such flight lines have limited coverage.

Synthetic Aperture Radar images suffer from 'speckle,' which is a noise-like variation in pixel values induced in the pixel amplitude as a result of self-interference that is intrinsic to radar operation. Speckle is reduced by averaging multiple pixels together, which results in tradeoff between speckle noise level and spatial resolution. Spatial resolution is also affected by the bandwidth of the SAR signal. A complication of air-borne low-altitude operation of the SAR is the effect of the variation in the incident angle of the radar signal over the image. The observed backscatter from the ground is a function of incidence angle, which produces a gradient in the image values that can complicate change detection. This issue can be mitigated by employing multiple overlapping swaths that provide incidence angle diversity. These also minimize gaps between the swaths. Strip-map flight lines with enough overlap to obtain 2 views of each point on the ground is an ideal setup for finding surface-level polar bears.

A racetrack data-collection approach that creates overlapping images provides multiple views at each potential bear location (Fig. 5; Cumming and Wong 2005). Wider look angles, higher elevations, faster flight speeds, and more efficient flight lines permit more land area imaged per hour of flight time. The trade-off is that higher elevations increase swath size but may also decrease penetration depth into snow because of the increased slant range and changes in the incidence angle of the observation. In an effort to optimize SAR clarity and area covered, we attempted to image each area of interest on a given day twice to help account for lost data and poor-quality data due to flight perturbations. We imaged 5.7 km^2 (2.2 mi^2) of land area/hour when flying at heights averaging 183 m (600 ft) above ground level. This figure includes time spent flying between flight lines that are several kilometers apart when the SAR was not operating. If flight lines are planned closer to each other, or in a racetrack pattern as in Figure 5, the area covered per unit time can be increased. Coverage rate also can be increased with fixed-wing aircraft because of their greater flight speed.

As it turned out, low cloud cover limited the maximum aircraft altitude to between 150 m (500 ft) and 450 m (1,500 ft), depending on the day. On 2 of the 3 testing days, we were able to fly with most of the flight lines at heights between 150 m (500 ft) and 215 m (700 ft). Unfortunately, on the third flight day, the cloud cover was too low and winds were too high, which resulted in cancellation of the flights planned for that day.

Bear locations

As previously noted, we selected Churchill as the experiment site because of the availability of many known bear locations in a small area, enabling us to test whether bears could be identified in SAR images. In Churchill during the time of the experiment, the bears were above ground and mobile. In order to confirm the bear location, they were first sighted from the ground. Many of the bears were close enough to the road networks for a team to record the Global Positioning System (GPS) coordinates of the bears they observed from trucks and tundra buggies. These coordinates were relayed to the team creating flight lines for the helicopter so they could include these areas in the planned flight paths. We also imaged areas where local experts said polar bears often rest, even if no bears had been specifically identified in that area by our team.

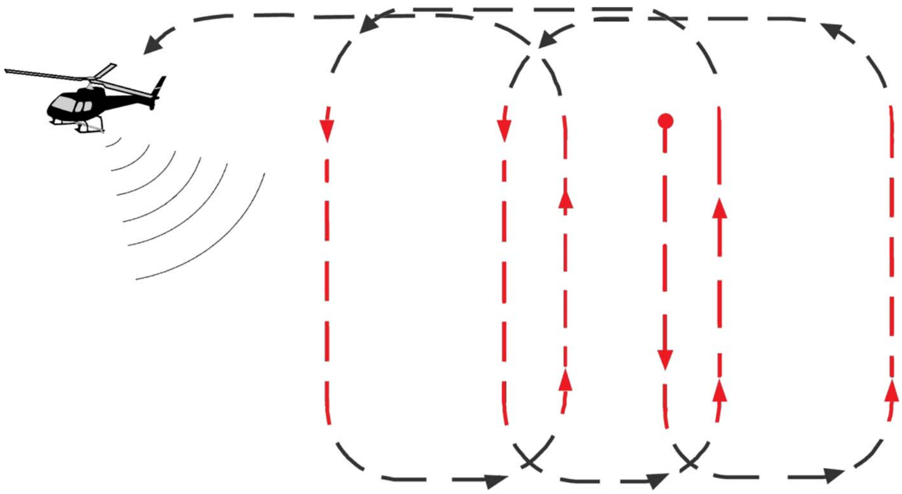

Fig. 5. Example of racetrack flight path for area mapping. The red dashed lines show the straight lengths where Synthetic Aperture Radar (SAR) data collection takes place.

These impromptu flight lines of areas with historically high bear activity were repeated on both days.

Experiment data

We collected a variety of data types in our pilot study and used them to create and analyze the images. The data included the SAR data, GPS position information, and imagery from the fodar. The first round of image production involved processing the raw SAR data into initial SAR images (Cumming and Wong 2005). We later processed these into precision images by Artemis Inc. (Haupauge, New York).

Processed SAR images comprise complex values where magnitude is proportional to the backscatter from the pixel for the particular polarization. An example gray-scale image for a particular polarization is shown in Figure 6; darker areas in the image typically represent flat, smooth surfaces that reflect away from the radar, whereas bright areas typically represent rough surfaces that backscatter brightly. Polar bears often appear as bright spots on a SAR image because of their large size, irregular shape, and high dielectric constant.

Image polarizations

Each SAR data collection included 4 transmit–receive polarization combinations. Separate images of each polarization combination as illustrated for a particular area are shown in Figure 7. Each polarization potentially highlights different features based on the scattering mechanisms of the underlying objects. Together, these 4 polarizations (vertical transmit, vertical receive—VV, horizontal transmit, horizontal receive—HH, vertical transmit, horizontal receive—VH, and horizontal transmit, vertical receive—HV) help reveal the 'full picture.' Certain features appear brighter in some polarizations and darker in others. The HV polarization channel appears to have experienced some hardware-based distortion with vertical streaks across the image, demonstrating the importance of having redundancy.

The different polarization images can be combined into a composite false-color image, as seen in Figure 8. Three polarizations (for example, HH, HV, and VV) are converted to an RGB image using a color map where each polarization is assigned a color (red, green, and blue). The resulting RGB image displays features that are common to each polarization (white) as well as features unique to each polarization (their respective color map color). In this case, a polar bear in the image shows up as white.

Change detection

One approach to identifying polar bears in SAR images is to employ change detection (also referred to as difference detection). In SAR, change detection images are taken of the same area at 2 different times and compared to identify features that have changed. This can be done using the phase and magnitude information in the SAR images, a technique termed coherent change detection, or just the backscatter magnitude, which is termed incoherent change detection (Moreira et al. 2013). Coherent change detection imposes strict requirements on the aircraft passes, so we have exclusively used incoherent change techniques in this paper. We note, however, that the satellite-based SAR

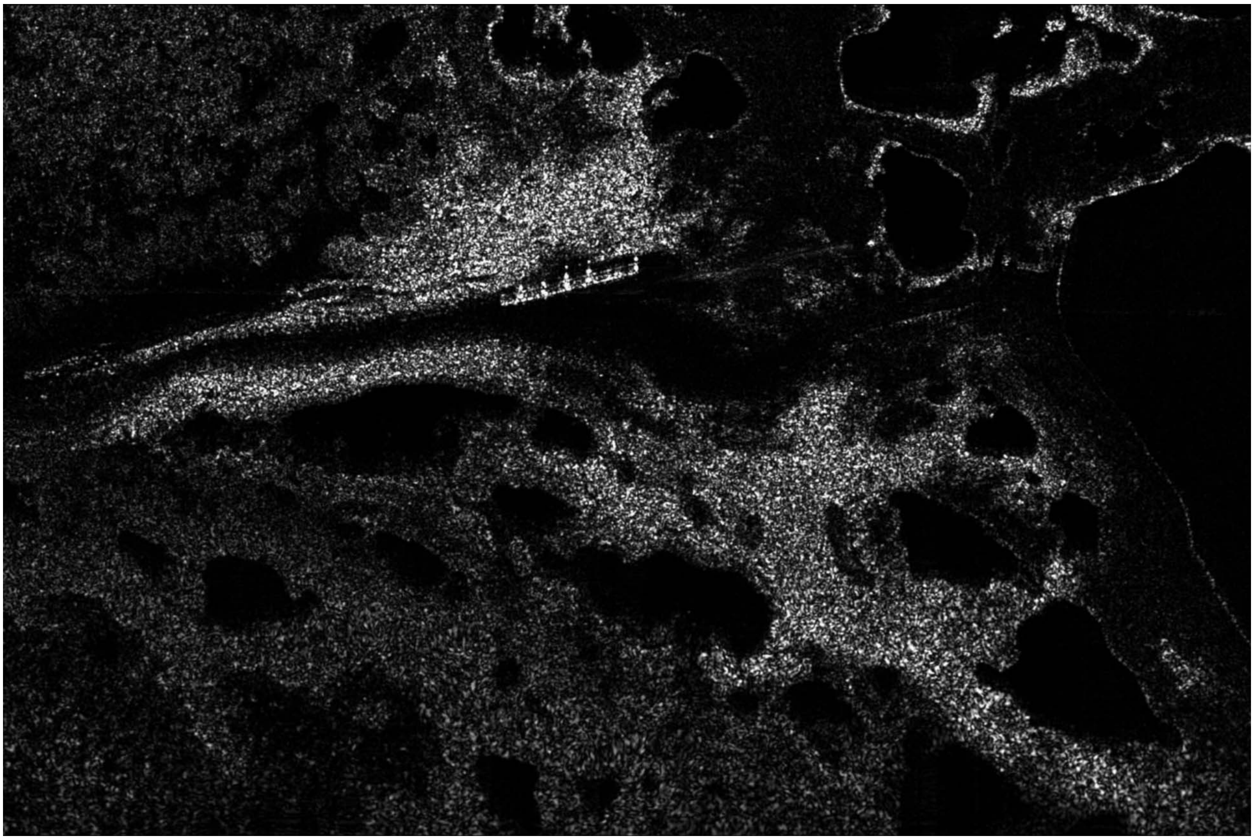

Fig. 6. Example of processed Synthetic Aperture Radar horizontal transmit, horizontal receive (SAR HH) -polarization image. Area covered is approximately 1 km × 1.25 km with a multilook pixel resolution of approximately 1 m.

coherent change detection has been successfully used in other studies (Stapleton et al. 2014, LaRue et al. 2015, LaRue and Stapleton 2018). For incoherent SAR change detection, the SAR backscatter images are first coregistered and then compared. Figure 1 illustrates an example of results in this study.

For polar bear identification, change detection involves imaging an area of interest prior to when bears are expected, and then imaging the area again after bears are expected. A difference image is then created from the 2 images, and a polar bear is identified as a new feature that has changed between the 2 time periods. This change detection approach enables filtering out of common static features (rocks, trees, etc.) in SAR images that make it difficult to distinguish the polar bear dens. Unfortunately, small changes resulting from surface movement resulting from freeze–thaw cycles can occur, which can occasionally cause false and/or missed detections.

There is value to both a manual and an automated approach to change detection. Manual change detection done by visual inspection of 2 images of the same area serves as validation that change detection can be used for finding bears. Ultimately, the process can be automated for large-scale surveys using constant false alarm (CFAR; Richards et al. 2010) and other techniques. Current research on applying machine learning techniques for change detection is promising but is not yet mature enough to reliably overcome speckle noise found in SAR images (Wang et al. 2022).

Synthetic Aperture Radar images that cover large land areas often have a wide range of pixel brightness. Noise and small changes in high brightness (backscatter) can mask the existence of local differences when performing change detection. Polar bears may exist as local maxima in a certain section of the image, but can be missed by change detection when global maxima outshine them. For this reason, it is helpful to separate larger images into smaller sections and run each section through the change detection process. If there is no significant signature in the local image, change detection will not identify any points

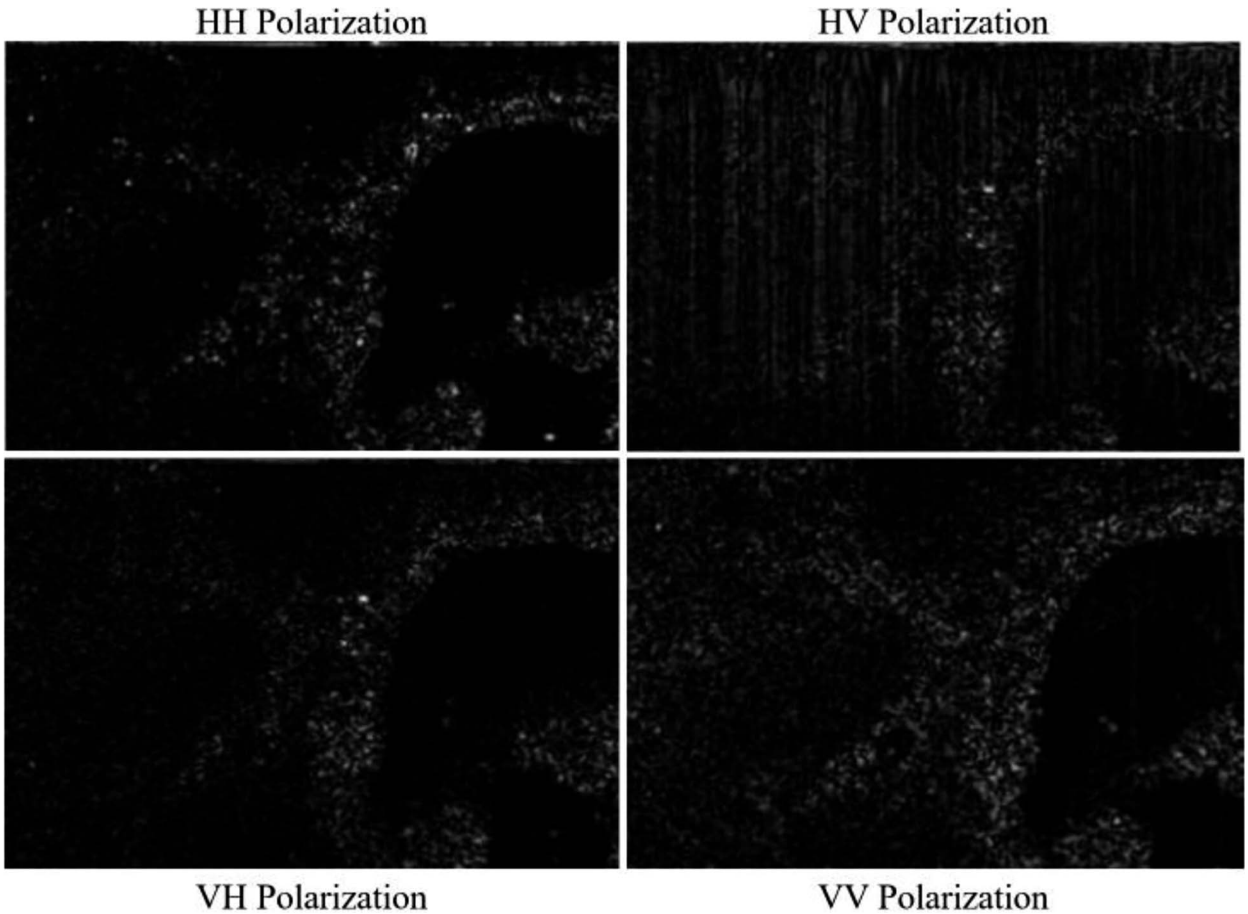

Fig. 7. Different polarization Synthetic Aperture Radar (SAR) images collected simultaneously. Each panel covers an area of approximately 100 m × 100 m with a multilook pixel resolution of approximately 1 m.

of interest. However, if there is a local maxima in the smaller section, change detection may now be able to identify this because it is no longer drowned out by a global maxima that is in a different section. Thus, when analyzing the SAR images, they should be divided into small regions for change detection. If the region is too large, polar bears may be missed. If the region is too small, then irrelevant local maxima that correspond with meaningless features in the landscape may be misidentified as polar bears. Machine learning can potentially be more precise in balancing this trade-off (Wang et al. 2022).

Results

The goal of the Churchill pilot study was to determine whether a polar bear's signature is visible in a SAR image. Human observation from tundra buggies and fodar were employed to locate polar bears during the study. Fodar was employed to confirm a bear's location and identify whether or not there was a corresponding signature in a SAR image, although in 2 cases the radar performed better than the fodar images. In the following, a particular example is shown, followed by a summary of the results.

Sample image analysis

We found a polar bear in Churchill on Day 1 located near a lake in some brush. The helicopter executed a flight line parallel to the bear and captured it in SAR images. On Day 2, we flew the same flight line and took another SAR image of the area once the bear had left. This set of images provided an excellent test case for applying change detection.

To illustrate, Figure 9 shows the fodar images from the helicopter on the 2 separate days. The fodar images are progressively zoomed in toward the polar bear's location. The bear appears as a white speck in

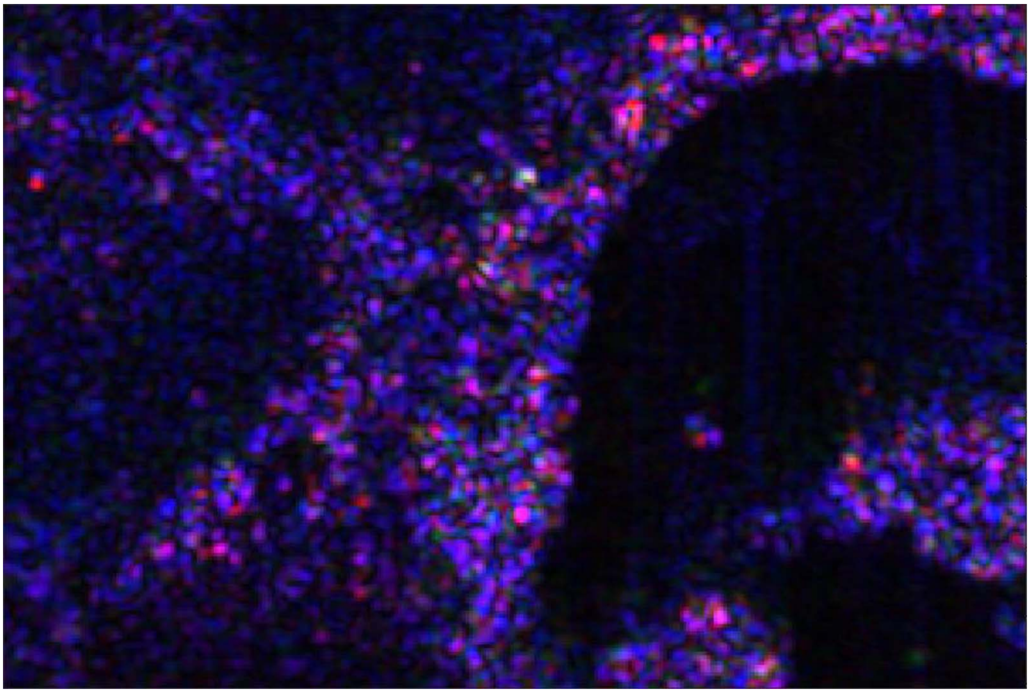

Fig. 8. Example of an enlarged false-color multipolarization image created from the images in Figure 7. A polar bear (*Ursus maritimus*) appears as the white spot in the upper center of the image.

the brush of the Day 1 photos. The bear is notably absent in the Day 2 photos.

The fodar images were then used to identify features in the SAR images. Figure 10 shows the fodar images and the corresponding SAR images cropped to display the same area. The features in the SAR images are matched to features in the fodar images using color markings. The polar bear's location is marked with a green circle when present, and a yellow circle when not present. As expected, the SAR signature at this location is different across the 2 days because of the presence of a polar bear on one of the days.

We used MATLAB to produce a difference image from the 2 SAR images. In the difference image in Figure 11, dark blue areas represent areas of similarity whereas yellow areas represent areas of difference. The colored markings from Figure 10 are included to help identify features.

The polar bear in the yellow circle appears as a yellow signature in the difference image. The yellow signature indicates a change between the 2 days—a promising result. However, there is another bright yellow signature produced by the rocks at the top right of the red trapezoid. This represents a false positive that was probably produced by deviations in the flight line. This challenge is addressed elsewhere. The other color-marked features are rocks and they appear as dark blue signatures. Light blue indicates that there was no change between the 2 images.

Summary

Prior to the Churchill flights, a ground crew in tundra buggies located 16 polar bears. Of those 16 bears, we were able to make helicopter flights over 11 of them at an altitude of 150–450 m (500–1,500 ft). During the flights, an observer in the Tundra Buggy recorded the position of the polar bear using a range finder, compass, and the vehicle GPS coordinates. Synthetic Aperture Radar and optical images were simultaneously collected for each flight. Good weather and lighting conditions enabled us to locate 9 of the 11 target bears in the fodar images. Using the SAR data we correctly identified 6 of 9 bears but could not unambiguously detect 3 of them. In the case of the other 2 bears, the SAR coverage placed the bears at the very edge of the images, so these cases were discarded as unusable.

Bear 1 was the best documented bear with 2 usable passes. Both passes had a corresponding fodar image confirming the bear's location. Bear 1 was first imaged on Day 1 of the study, then again on Day 2. Change detection for this polar bear is discussed below. Two

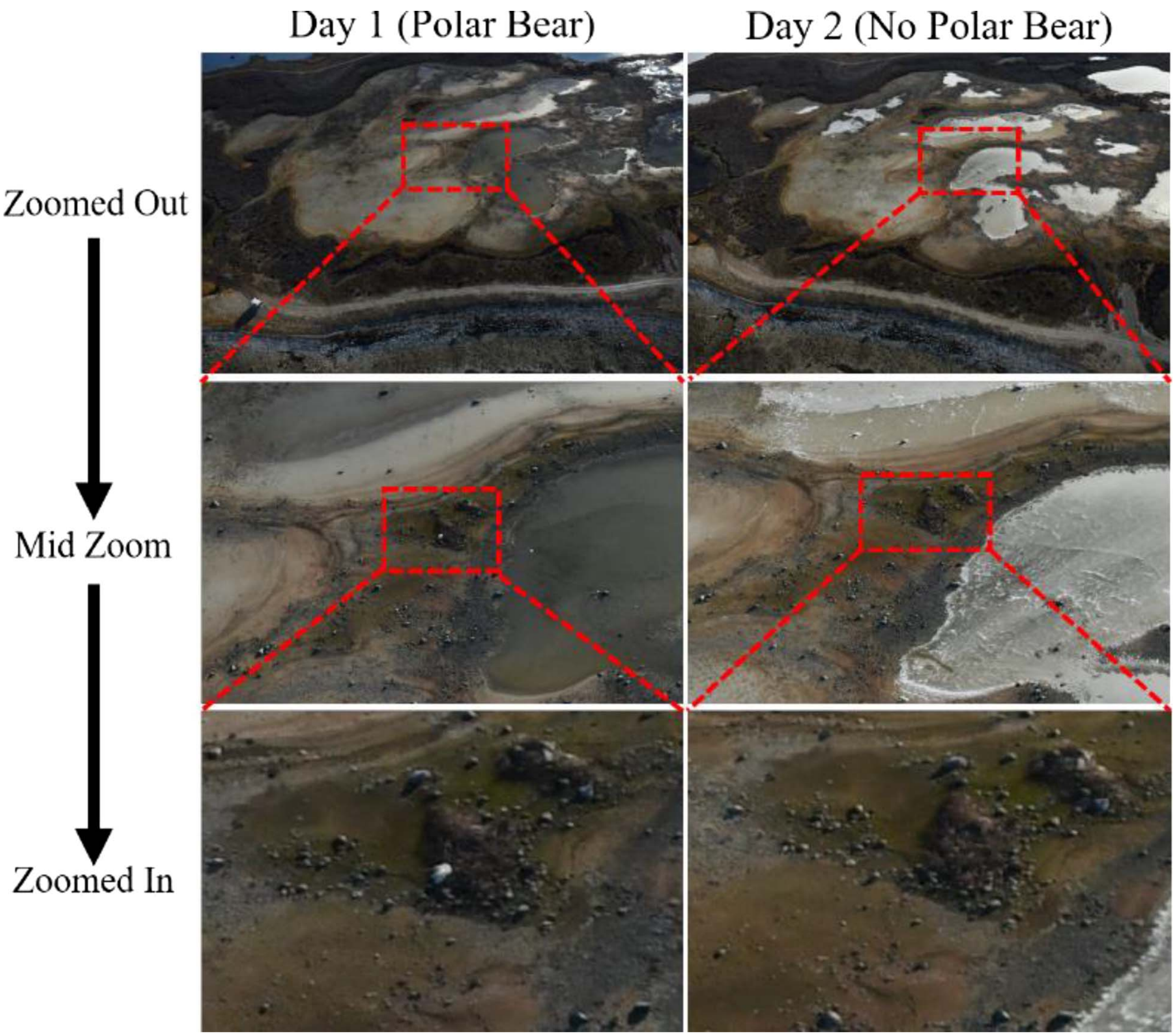

Fig. 9. Fodar comparison of a location used for change detection. Fodar images of the same land area are zoomed in to show the presence of a polar bear (*Ursus maritimus*) on Day 1 and the lack of a polar bear on Day 2.

bears were captured in SAR images and validated by ground truth from tundra buggies, but could not be identified in the corresponding fodar images.

The single largest challenge in identifying polar bears in the SAR images prior to applying change detection processing was the difficulty in differentiating them from polar bear-sized rocks. As discussed earlier, the use of change detection techniques ameliorates this issue.

Discussion

In this section we consider some of the challenges in using SAR to detect polar bears in our study.

Adherence to flight lines

Change detection requires flying the same flight line on different occasions. It is particularly important that the flight line is reproduced as closely as possible to allow the before and after images to be easily correlated. (We note that coherent SAR change detection has tighter requirements.) Small differences in angle and deviations from the flight line can affect how objects backscatter and introduce false differences in the 2 SAR images. Hence, using repeatable flight lines flown in good weather by an experienced pilot or automated drone are essential. Advanced SAR image processing techniques that include motion

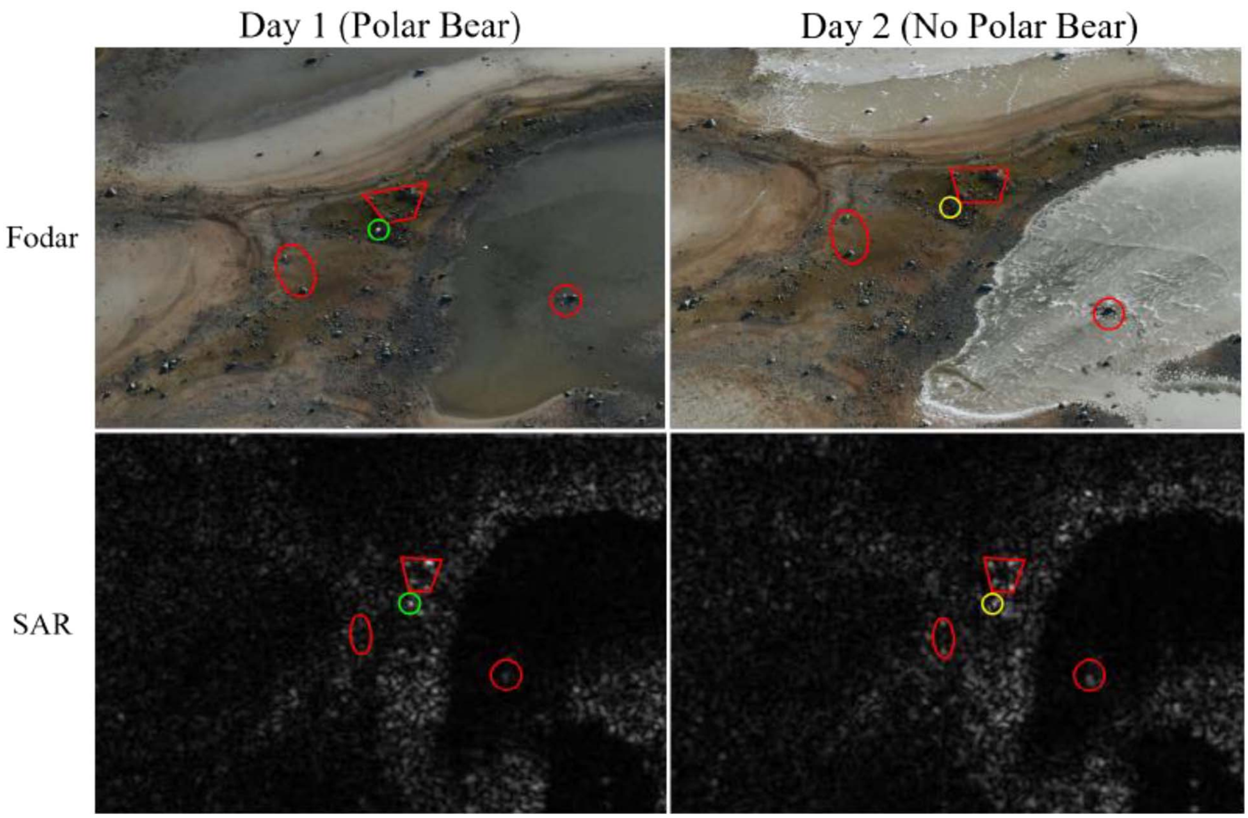

Fig. 10. Change Detection and Feature Matching. The bottom row shows Synthetic Aperture Radar (SAR) images taken at 2 different days while the top row shows fodar images. The colored shapes mark corresponding features in each image. The polar bear (*Ursus maritimus*) is circled in green on the left, with the area where it was on the next day circled in yellow. Note the differences in the viewing geometry of the fodar and SAR images. The SAR images are more map-like (i.e., in ground coordinates) than the projected images because of the nature of the SAR imaging process. Also note that change in color of the water feature on the right side of the fodar images that is due to a combination of changes in lighting conditions and surface freezing, whereas the SAR image is unaffected.

compensation and autofocus processing can improve the image quality but have their limitations. These issues are less pronounced for satellite SAR systems but are offset by limited resolution and coverage.

Figure 12 illustrates the effects of variations in flight geometry. In this case, the same basic flight path was followed on 2 separate days. The resulting difference image shows a large yellow difference at the Tundra Buggy Lodge. Careful inspection shows variations in positions resulting from slight deviations in the flight path that affects the look angles of the images. This is evident in the 2 fodar images and the SAR images that create a bright false positive in the difference image. This large signal can drown out the smaller differences corresponding to a polar bear presence.

Rocky terrain

The terrain of polar bear environments can vary, making this challenge dependent on region. One example is the case of the Alaska North Slope, where polar bears are found in relatively flat areas where the ground is mostly peat, while in Churchill, the environment is very rocky (Shilts and Boydell 1974). Rocks with a cross-sectional areas >0.7 m^2 can effectively camouflage the polar bear's signature in SAR images.

The presence of liquid water changes the rock's dielectric constant (Olhoeft 1981). We hypothesize that large, wet rocks have a radar backscatter response that is similar to that of a polar bear. If temperatures are far below 0°C for a sufficient period of time, the water inside

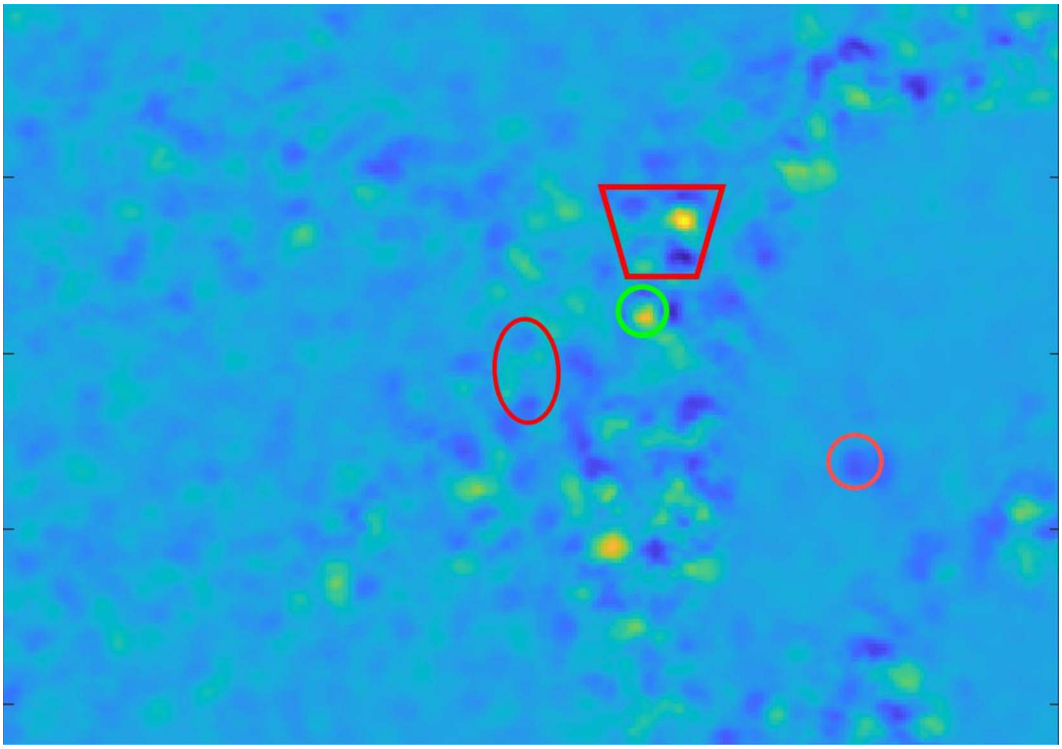

Fig. 11. Mean scaled difference image corresponding to Figure 10. The polar bear (*Ursus maritimus*) position is circled in green. The red shapes correspond to the areas in Figure 10.

the rocks freezes, reducing the dielectric constant and radar backscatter response of the rocks (Ulaby and Long 2014). Freezing temperatures also decrease the water saturation of the ice and snow that surrounds the bear dens. When the liquid water concentration is low in snow and ice, they are nearly transparent to a radar of sufficient wavelength, though there may be some backscatter interface layers (Ulaby and Long 2014).

Stationary objects like rocks can be filtered out using change detection. In practice, however, rocks may shift and so minimizing the time window between the first and second pass over an area makes change detection more effective. This should be explored in greater depth to determine ideal SAR data collection times.

Figure 13 shows an example in Churchill where a polar bear is imaged on a rocky shore. Colored markings have been added to the images to show corresponding features in the fodar and SAR images. The polar bear is circled in green. Through visual inspection of the fodar image, it is difficult to distinguish the polar bear from all of the similarly colored, large rocks surrounding it. Furthermore, the rocky shore introduces backscatter into the corresponding SAR image, making it nearly impossible to distinguish the polar bear's signature from the rocks.

Recommendations for future experiments

The pilot study experiment in Churchill, despite difficulties with the terrain and weather conditions, proved that a polar bear signature can be visible in a SAR image and detected using change detection algorithms. However, the difficulties in discriminating polar bears from rocks suggest that further experimentation is needed to fully evaluate the efficacy of SAR as a polar bear den detection technology.

We suggest that future SAR experiments for polar bear den detection be conducted in environments such as the Alaska North Slope. The terrain in Alaska is mostly composed of gravel-sized rocks and is relatively free of polar-bear-sized rocks that negatively affected the results of our study in Churchill.

The work in Churchill exclusively focused on bears above the surface. Researchers should consider conducting future experiments on both surfaced bears and denned bears to test radar penetration and the visibility of dens suspended in snow. This allows for a more conclusive

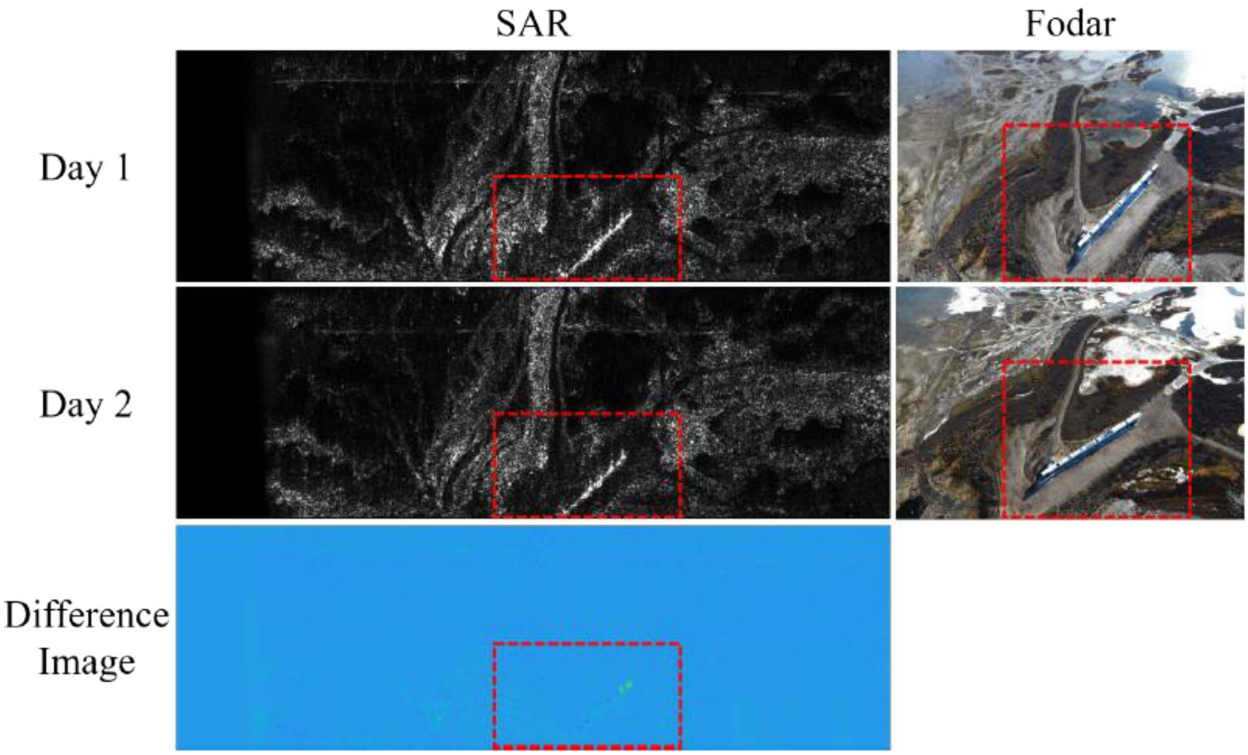

Fig. 12. Illustration of the challenges due to deviation in flight line and look angle. While the Synthetic Aperture Radar (SAR) images on Day 1 and Day 2 appear to capture the same area, the corresponding fodar images show a difference in the approach of the helicopter, as clearly seen in the angle of the Tundra Buggy Lodge. In change analysis, the Tundra Buggy Lodge shows as a yellow diagonal line, even though the Lodge is in the same location and orientation on both days and should ideally be filtered out by change detection.

evaluation of polar bear and polar bear den detection using SAR.

Our SAR imaging study was limited to the single frequency range of the available radar system (i.e., L-band). We were unable to test the effect of different radar bands for detecting polar bears and dens. Other frequencies may provide additional contrast between bear and terrain. In particular, simultaneous collection of SAR imagery at multiple frequencies is suggested as a way to further improve detection performance.

Change detection combined with machine learning is a promising tool for increasing den detection accuracy. Recent research shows that machine learning has the potential to conquer many of the obstacles outlined in this paper, such as the inherent noise levels in SAR images and false-positive bright spots in change detection due to flight line differences (Wang et al. 2022). Machine learning models generally require a large number of labeled images to learn from. Therefore, conducting more experiments with known bear locations to gather more labeled training data for a machine learning model may be required before attempting to use a model to identify unknown den locations.

Conclusion

The purpose of the Churchill pilot study was to determine whether polar bears have radar signatures visible in SAR images. We confirmed that polar bears can be detected in SAR images and were able to identify ~66% of the bears in the SAR images collected during the brief Churchill study period. This is a promising result and we found change detection to be a particularly effective approach. We recommend further research into SAR applications to differentiate between polar bears and other terrain features. Future research is recommended, particularly to increase the sample set size and validate detection of denning polar bears. Further, we believe that combining air-borne SAR

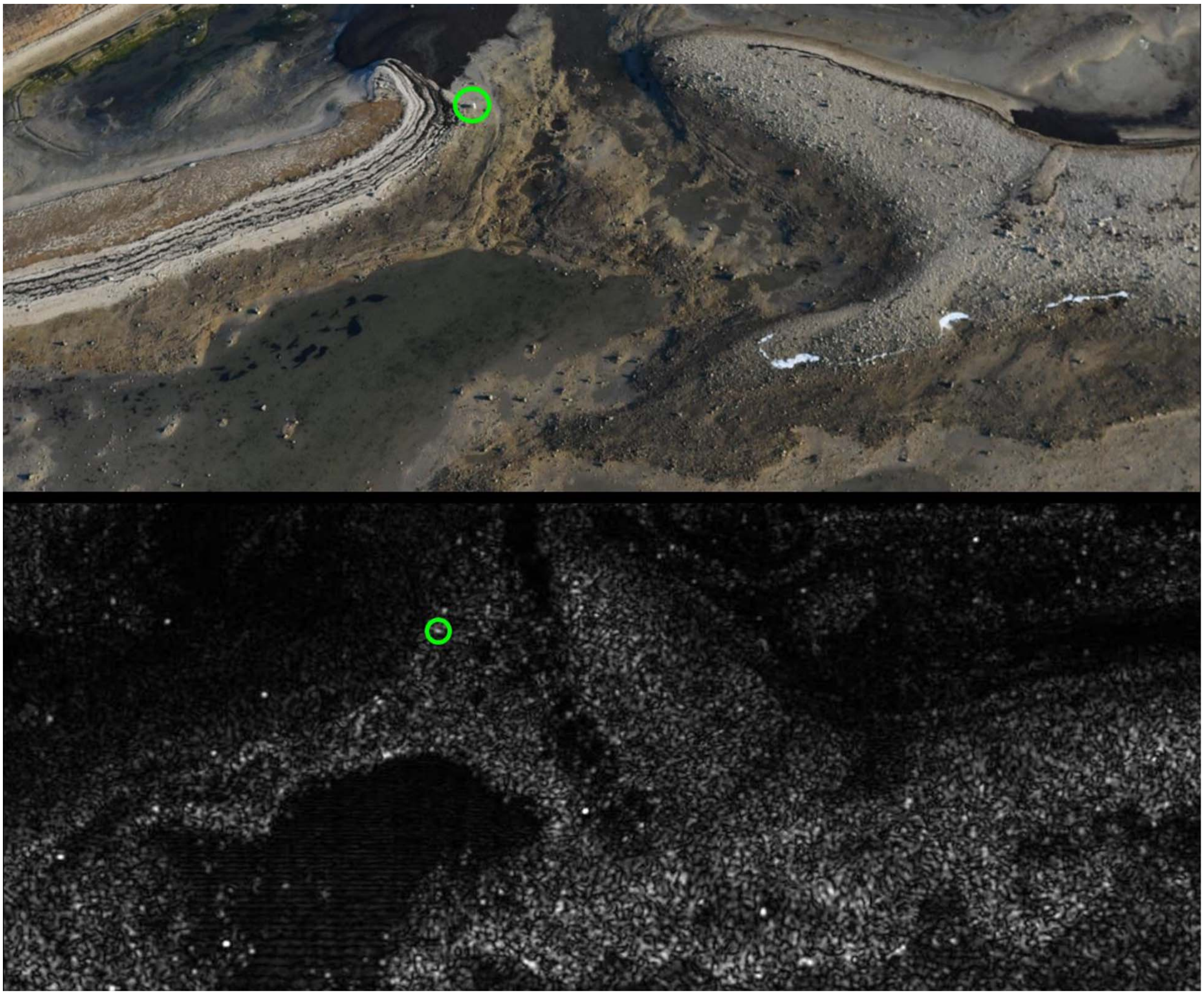

Fig. 13. Terrain effects on backscatter compared with a polar bear (*Ursus maritimus*). Top panel is the fodar image. Bottom panel is Synthetic Aperture Radar (SAR) image. Polar bear in both images is circled in green.

and FLIR can exploit the strengths of each approach in order to find and locate polar bears more accurately.

Acknowledgments

This research has been a collaborative effort among several invested parties, each of whom was essential to the success of the experiment. Our thanks to K.T. Miller and Polar Bears International for organizing each participating party and devoting extensive time to fundraising for shipping costs, travel, helicopter time, and other costs associated with the experiment. We particularly thank Artemis, Inc., Haupauge, New York, USA, for supporting expedited radar repairs, prioritized tech support, processing of Synthetic Aperture Radar (SAR) data, and preparing the SAR unit for operation at Churchill. We would like to thank the Associate Editor and reviewers for their help and thoughtful comments as we prepared this manuscript.

Literature cited

AMSTRUP, S., G. YORK, T. MCDONALD, R. NIELSON, AND K. SIMAC. 2009. Detecting denning polar bears with forward-looking infrared (FLIR) imagery. BioScience 54:337–344. https://doi.org/10.1641/0006-3568(2004)054[0337:DDPBWF]2.0.CO;2

CUMMING, I.G., AND F.H. WONG. 2005. Digital processing of synthetic aperture radar data—Algorithms and implementations. Artech House, Boston, Massachusetts, USA.

DEOCHER, A.E., AND I. STIRLING. 1990. Distribution of polar bears (*Ursus maritimus*) during the ice-free period in western Hudson Bay. Canadian Journal of Zoology 68(7): 1395–1403.

DOERRY, A.W. 2008. Reflectors for SAR performance testing. Sandia National Laboratory Technical Report SAND2008-0396, Albuquerque, New Mexico, and Livermore, California, USA. https://doi.org/10.2172/929123, Accessed 12 May 2023.

DURNER, G., AND T. ATWOOD. 2018. A comparison of photograph-interpreted and IfSAR-derived maps of polar bear denning habitat for the 1002 Area of the Arctic National Wildlife Refuge. U.S. Geological Survey Open-File Report 2018-1083. Alaska Science Center. https://doi.org/10.3133/ofr20181083. Accessed 12 May 2023.

DYCK, M.G., AND R.K. BAYDACK. 2004. Vigilance behaviour of polar bears (*Ursus maritimus*) in the context of wildlife-viewing activities at Churchill, Manitoba, Canada. Biological Conservation 116(3):343–340.

GARTHWAITE, M.C., S. NANCARROW, A. HISLOP, M. THANKAPPAN, J.H. DAWSON, AND S. LAWRIE. 2015. The design of radar corner reflectors for the Australian geophysical observing system: A single design suitable for InSAR deformation monitoring and SAR calibration at multiple microwave frequency bands. Record 2015/003. Geoscience Australia, Canberra, Australian Capital Territory, Australia. http://dx.doi.org/10.11636/Record.2015.003, Accessed 12 May 2023.

LARUE, M., AND S. STAPLETON. 2018. Estimating the abundance of polar bears on Wrangel Island during late summer using high-resolution satellite imagery: A pilot study. Polar Biology 41:2621–2626.

———, ———, C. PORTER, S. ATKINSON, T. ATWOOD, M. DYCK, AND N. LECOMTE. 2015. Testing methods for using high-resolution satellite imagery to monitor polar bear abundance and distribution. Wildlife Society Bulletin 39: 772–779. https://doi.org/10.1002/wsb.596.

LI, C., J. ZHAO, J. YIN, G. ZHANG, AND X. SHAN. 2010. Analysis of RCS characteristic of dihedral corner and triangular trihedral corner reflectors. Pages 40–43 in 2010 5th international conference on computer science & education. DOI: 10.1109/ICCSE.2010.5593647, Accessed 12 May 2023.

MOREIRA, A., P. PRATS-IRAOLA, M. YOUNIS, G. KRIEGER, I. HAJNSEK, AND K. PAPATHANASSIOU. 2013. A tutorial on synthetic aperture radar. IEEE Geoscience and Remote Sensing Magazine 1:6–43. https://doi.org/10.1109/MGRS.2013.2248301

NOLAN, M., C. LARSEN, AND M. STURM. 2015. Mapping snow depth from manned aircraft on landscape scales at centimeter resolution using structure-from-motion photogrammetry. The Cyrosphere 9:1448–1449. https://tc.copernicus.org/articles/9/1445/2015/tc-9-1445-2015.pdf

OLHOEFT, G. 1981. Electrical properties of rocks. Pages 257–330 in Y.S. Touloukian, Y.S. Judd, and R.F. Roy, editors. Physical properties of rocks and minerals. Volume 2. McGraw-Hill, New York, New York, USA.

PEDERSEN, N., T. BRINKMAN, R. SHIDELER, AND C. PERHAM. 2020. Effects of environmental conditions on the use of forward-looking infrared for bear den detection in the Alaska Arctic. Conservation Science and Practice 2(7): e215. https://doi.org/10.1111/csp2.215

REGEHR, E.V., N.J. LUNN, S.C. AMSTRUP, AND I. STIRLING. 2010. Effects of earlier sea ice breakup on survival and population size of polar bears in western Hudson Bay. Journal of Wildlife Management 71(8):2673–2683.

RICHARDS, M.A., J.A. SCHEER, AND W.A. HOLM. 2010. Principles of modern radar. Volume I: Basic principles. SciTech, Raleigh, North Carolina, USA.

ROH, N., S. OH, AND D. PARK. 2020. Aerodynamic characteristics of helicopter with ducted fan tail rotor in hover under low-speed crosswind. International Journal of Aerospace Engineering 2020:Article ID 7059209. https://doi.org/10.1155/2020/7059209

SHILTS, W., AND A. BOYDELL. 1974. Terrain mapping in the Churchill Chesterfield Inlet corridor. Geological Survey of Canada 74-1A. https://doi.org/10.4095/103255, Accessed 12 May 2023.

SMITH, T.S., S.C. AMSTRUP, J. KIRSCHHOFFER, AND G. YORK. 2020. Efficacy of aerial forward-looking infrared surveys for detecting polar bear maternal dens. PLoS One 15(2):e0222744. https://journals.plos.org/plosone/article?id=10.1371/journal.pone.0222744.

STAPLETON, S., M. LARUE, N. LECOMTE, S. ATKINSON, D. GARSHELIS, C. PORTER, AND T. ATWOOD. 2014. Polar bears from space: Assessing satellite imagery as a tool to track arctic wildlife. PLoS ONE 9(7):e101513.

STIRLING, I., N. LUNN, J. IACOZZA, C. ELLIOTT, AND M. OBBARD. 2004. Polar bear distribution and abundance on the southwestern Hudson Bay coast during open water season, in relation to population trends and annual ice patterns. Arctic 57(1):15–26.

ULABY, F.T., AND D.G. LONG. 2014. Microwave radar and radiometric remote sensing. The University of Michigan Press, Ann Arbor, Michigan, USA.

U.S. DEPARTMENT OF TRANSPORTATION, FEDERAL AVIATION ADMINISTRATION. 2023. Section 4-4-6: Air traffic control/ATC clearances and aircraft separation/Special VFR clearances. Pages 245–246 in Aeronautical information manual. Federal Aviation Administration. https://www.faa.gov/air_traffic/publications/media/aim_basic_dtd_4-20-23.pdf. Accessed 12 May 2023.

WANG, J., F. GAO, J. DONG, Q. DU, AND H. LI. 2022. Change detection from synthetic aperture radar images via dual path denoising network. IEEE Journal of Selected Topics in Applied Earth Observations and Remote Sensing 15:1–2, 12.

WOODRUFF, S.P., J.J. BLANK, S.S. WISDOM, R.R. WILSON, G. M. DURNER, T.C. ATWOOD, C.J. PERHAM, AND C.H.M. POHL. 2022. Evaluating the efficacy of aerial infrared surveys to detect artificial polar bear dens. Wildlife

Society Bulletin 46(3):e1324. https://doi.org/10.1002/wsb.1324

Zyl, J.V., and Y. Kim. 2011. Synthetic Aperture Radar polarimetry. Jet Propulsion Laboratory Space Science and Technology Series, California Institute of Technology, La Cañada Flintridge, USA. John Wiley & Sons, Hoboken, New Jersey, USA. https://onlinelibrary.wiley.com/doi/pdf/10.1002/9781118116104.fmatter. Accessed 12 May 2023.

Received: December 3, 2022
Accepted: April 3, 2023
Associate Editor: M. Obbard